

Supplemental Material

Multi-Modality Imaging in Survivors of COVID-19

Singh T BM BMedSci*,^{1,2,3} Kite TA BM BS BMedSci*,⁶ Joshi S MBBS,^{1,2,3} Spath NB MBBS,^{1,2,3} Kershaw L PhD,^{3,4} Baker AH BSc PhD,¹ Jordan H MBChB FGRCA FFICM,⁵ Gulsin GS MBChB BSc PhD,⁶ Williams MC MBChB PhD,^{1,3} van Beek EJ MD PhD,¹ Arnold RJ BMBCh DPhil,⁶ Semple SI MSc PhD,^{1,3} Moss AJ MBBS PhD,⁶ Newby DE DM PhD,^{1,2,3} Dweck MR MBChB PhD,^{1,2,3} McCann GP MBChB MD⁶

1. BHF/University Centre for Cardiovascular Science, University of Edinburgh, UK
2. Edinburgh Heart Centre, Royal Infirmary of Edinburgh, UK
3. Edinburgh Imaging, University of Edinburgh, UK
4. Centre for Inflammation Research, University of Edinburgh, UK
5. Department of Anaesthesia, Critical Care and Pain Medicine, Royal Infirmary of Edinburgh, UK
6. Department of Cardiovascular Sciences, University of Leicester and NIHR Leicester Biomedical Research Centre, Glenfield Hospital, UK

* Authors contributed equally

Supplemental Methods:

Exclusion criteria:

High degree atrioventricular block, torsades de pointes, prolonged QTc interval, liver failure, calcium-channel blockers or digoxin, renal failure, New York Heart Association class IV heart failure, and pregnancy.

Quick COVID-19 Severity Index:

The Quick COVID-19 Severity Index (qCSI) has been validated to risk-stratify patients with COVID-19 during the first 24 hours of hospital admission and assess their risk of critical illness.¹ The formula is based on 3 variables: respiratory rate (breaths/min), pulse oximetry (lowest value recorded, %) and O2 flow rate (L/min).

The score and its associated risk of critical illness is shown below:

qCSI	Risk Level	Risk of Critical Illness at 24 hours (%)
<3	Low	4
4-6	Low-intermediate	30
7-9	High-intermediate	44
10-12	High	57

Late gadolinium-enhancement

Haematocrit was measured on the day of scanning and was used to calculate global extracellular volume fraction . Endocardial and epicardial borders were manually defined on all the conventional short-axis images for volumetric and wall motion measurements and were then copied to all corresponding LGE and T1 map sequences for analysis with minimal manual adjustments. After contouring, an additional epicardial and endocardial offset of 20% was applied automatically to minimise tissue interface for all T1 map analyses and artefact was excluded manually for a minority of cases. Regions of interest (ROIs) were determined using the standard 16-segment cardiac model with septal native T1 values. For patients with previous

myocardial infarction or a new diagnosis of infarction, region of interest (ROIs) was defined in the remote myocardium. For those with a non-ischaemic pattern of late-enhancement native T1 was defined in the septal wall.

Manganese-enhanced magnetic resonance imaging

For patients with COVID-19, a single short-axis slice was then identified to represent pathological myocardium, guided by the late gadolinium enhancement, native T1 maps and cine images. For all participants with no obvious abnormality, a single mid-ventricular short-axis slice was selected. A single short-axis T1 mapping was then performed at this slice location every 2.5 min for 30 min after starting manganese contrast infusion, at which point a full short-axis shortened modified Look-Locker inversion recovery stack was repeated post-contrast (**Supplemental Figure 1**).^{2,3}

Coronary Computed Tomography Angiography

Patients with a heart rate over 60 /min received intravenous metoprolol and all patients received sublingual glyceryl trinitrate prior to imaging. CCTA imaging was reviewed on a dedicated post processing workstation (Vitrea Advanced, v6.9.68.1, Vital Images, US) by experienced observers (MCW, EJRB). Obstructive coronary artery disease was defined as a luminal cross-sectional area stenosis of >70% in a major epicardial vessel or >50% in the left main stem. Prognostically significant coronary artery disease was defined as left main stem stenosis >50%, three-vessel disease or two-vessel disease including stenosis of the proximal left anterior descending coronary artery. Lung windows were reviewed for pulmonary COVID-19 involvement or persistent parenchymal lung abnormalities (atelectasis/scarring or ground glass opacification).⁴

Power Calculation:

We have a number of exploratory end-points and our initial sample size calculation was based on our manganese-enhanced magnetic resonance imaging. To calculate the initial sample size, we have used the gradient of T1 values as a measure of calcium uptake and utilisation.² We have found that the mean gradient of change in T1 over 30 minutes in healthy volunteer myocardium was -3.749 ± 1.015 , compared to -2.540 ± 0.583 in non-ischaemic cardiomyopathy. For detecting a conservative difference in rate of change of 5%, we required at least 15 subjects at 90% power and two-sided $P < 0.05$.

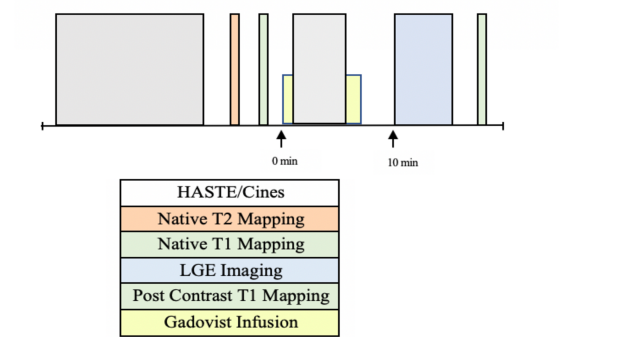
References:

1. Haimovich AD, Ravindra NG, Stoytchev S, Young HP, Wilson FP, Dijk D van, Schulz WL, Taylor RA. Development and Validation of the Quick COVID-19 Severity Index: A Prognostic Tool for Early Clinical Decompensation. *Ann Emerg Med* 2020;
2. N.B. Spath,*†, T. Singh†, G. Papanastasiou, L. Kershaw, A.H. Baker, R.L. Janiczek, G.S. Gulsin, M.R. Dweck, G. McCann, D.E. Newby and SIS. Manganese-enhanced magnetic resonance imaging in dilated cardiomyopathy and hypertrophic cardiomyopathy. *Eur Heart J Cardiovasc Imaging* 2020;**00**:1–10.
3. Spath NB, Lilburn DML, Gray GA, Page LM Le, Papanastasiou G, Lennen RJ, Janiczek RL, Dweck MR, Newby DE, Yang PC, Jansen MA, Semple SI. Manganese-Enhanced T1 Mapping in the Myocardium of Normal and Infarcted Hearts. *Contrast Media Mol Imaging* 2018;e9641527.
4. Simpson S, Kay FU, Abbata S, Bhalla S, Chung JH, Chung M, Henry TS, Kanne JP, Kligerman S, Ko JP, Litt H. Radiological Society of North America Expert Consensus Document on Reporting Chest CT Findings Related to COVID-19: Endorsed by the Society of Thoracic Radiology, the American College of Radiology, and RSNA.

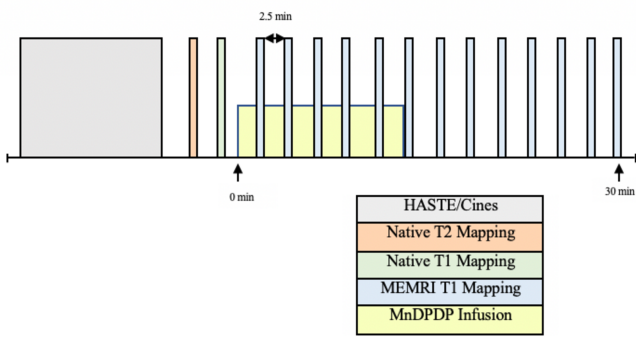
Radiol Cardiothorac Imaging 2020;**2**:e200152.

Supplemental Figure 1: MR protocol

Gadolinium-Enhanced MR protocol:

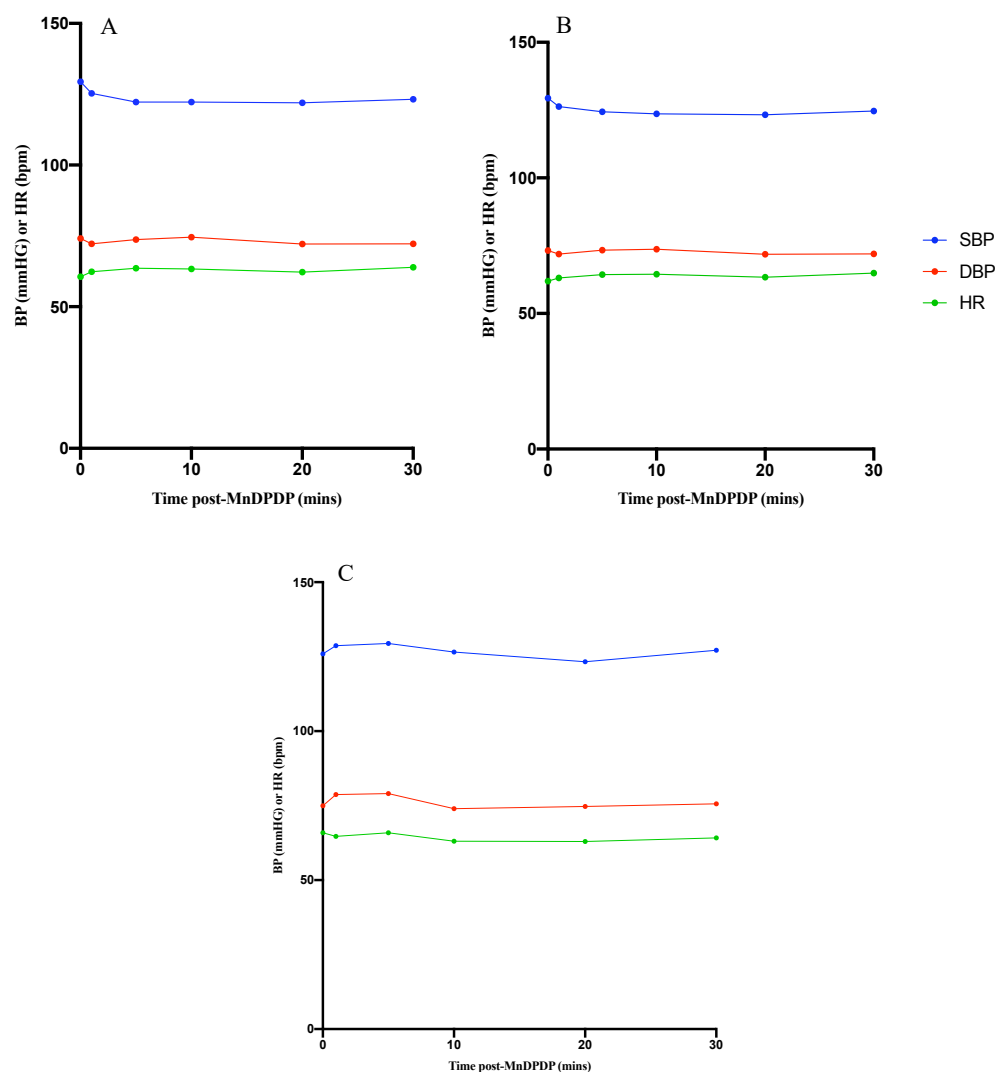


Manganese-Enhanced MR protocol:



MnDPDP, manganese dipyridoxyl diphosphate, LGE, Late gadolinium enhancement, MR, Magnetic Resonance

Supplemental Figure 2 Haemodynamic and Electrocardiography monitoring with MEMRI
Blood pressure and heart rate after administration of MnDPDP in healthy volunteers, (A) matched volunteers (B) and patients (C).



MEMRI, Manganese-enhanced magnetic resonance imaging, MnDPDP, manganese dipyridoxyl diphosphate, SBP, systolic blood pressure, DBP, diastolic blood pressure, HR, heart rate.

Supplemental Table 1: Laboratory biomarkers

Laboratory Findings	Recovered COVID-19 (n=52)
Peak white-cell count (x10 ⁹ /L)	11.6 (4 - 11)
Peak neutrophil count (x10 ⁹ /L)	7.9 (2 - 7.5)
Lowest lymphocyte count (x10 ⁹ /L)	0.94 (1.5 - 4.5)
Peak C-reactive protein (mg/L)	150 (0 – 5)
Peak D-dimer (ng/L)	1563 (0 - 230)
Peak ferritin (ug/L)	1058 (20- 300)
Peak procalcitonin (ug/L)	0.22 (>0.15)
Elevated troponin (>99 th percentile)	17
Peak high-sensitivity troponin I (ng/L)	1068 (female<16, male:<34)

n (reference range)

Supplemental Table 2: Electrocardiographic and Echocardiographic Findings

	Recovered COVID-19 (n=52)
ECG changes	16(31)
Rhythm disturbance	4 (25)
ST segment deviation	4 (25)
T wave deviation	10(50)
Echocardiogram	10 (19)
Right ventricle dilatation	6 (60)
Right ventricle dysfunction	1 (10)
Left ventricle dilatation	2 (20)
Left ventricle dysfunction	3 (30)
Regional wall motion abnormalities	3 (30)

n (%)

Supplemental Table 3: RV insertion point late-gadolinium enhancement.

	Patients with COVID-19 (n=52)	Matched Co-Morbidity-Matched Volunteers (n=26)	Healthy Volunteers (n=10)
Presence of right ventricular insertion point LGE	18 (35)	10 (38)	1 (10)

LGE, Late gadolinium enhancement

n (%)

Supplemental Table 4: Subgroup analysis of magnetic resonance imaging findings

	Matched Volunteer (n=26)	Recovered COVID-19 (n=52)					
		Severe COVID-19 (n=27)	P value	Myocardial Injury (n=17)	P value	Ongoing Symptoms (n=20)	P value
LV Ejection Fraction, mean \pm SD (95% CI) (%)	61.6 \pm 9.9 (56.1-65.2)	58.3 \pm 10.1 (54.3-62.3)	0.35	57.5 \pm 13.1 (52.5-64.6)	0.08	57.9 \pm 9.2 (53.5-62.3)	0.35
RV Ejection Fraction, mean \pm SD (95% CI) (%)	59.3 \pm 4.9 (51.0-66.5)	52.2 \pm 10.2 (48.1-56.2)	0.0012	51.4 \pm 2.1 (47.4-55.4)	0.0017	49.0 \pm 6.5 (45.9-52.2)	<0.0001
Late Gadolinium Enhancement pattern	9 (35)	9 (33)		9 (53)		7 (35)	
Ischaemic	5 (56)	5 (56)		6 (67)		5 (71)	
Non-Ischaemic	4 (44)	4 (44)		3 (33)		2 (29)	
Native T1-Septum, mean \pm SD (95% CI) (ms)	1227 \pm 51** (1208-1246)	1223 \pm 46* (1202-1243)	0.99	1221 \pm 24* (1190-1251)	0.88	1230 \pm 23* (1202-1276)	0.96
Global T1-midventricular, mean \pm SD (95% CI) (ms)	1208 \pm 33** (1191-1228)	1210 \pm 37* (1198-1232)	0.81	1208 \pm 42* (1190-1225)	0.91	1228 \pm 28* (1200-1274)	0.89
Extracellular Volume, mean \pm SD (95% CI) (%)	31 \pm 4 (29.6-32.1)	30 \pm 2 (27.7-30.5)	0.99	32 \pm 2 (27.0-34.3)	0.66	30 \pm 5 (27.7-33.1)	0.74
T2, mean \pm SD (95% CI) (ms)	37.3 \pm 4.6 (35.9-38.6)	38.4 \pm 1.9 (37.6-39.2)	0.94	38.9 \pm 3.1 (37.1-40.1)	0.51	38.7 \pm 2.0 (37.8-39.7)	0.85
Manganese Influx constant, mean \pm SD (95% CI) (Ki/mL/100 g/min)	6.9 \pm 0.9* (6.5-7.3)	6.7 \pm 1.1 (6.1-7.3)	0.46	6.2 \pm 0.5* (5.9-6.5)	0.22	6.3 \pm 0.8* (5.6-6.8)	0.62

n (%) or mean \pm standard deviation (95% CI)

*n= 23

**n= 20

